

UBQLN4 is an ATM substrate that stabilizes the anti-apoptotic proteins BCL2A1 and BCL2L10 in mesothelioma

Fang Liu¹ , RunSang Pan², HongYu Ding³ , LiLing Gu^{1,4,5}, Yun Yang¹, ChuanYin Li³, YongJie Xu⁵, Ronggui Hu³, Hui Chen⁵, XiangYan Zhang⁵ and YingJie Nie⁵

1 Medical College, Guizhou University, Guiyang, China

2 GuiYang Maternal and Child Hospital, Guiyang, China

3 State Key Laboratory of Systems Biology, CAS Center for Excellence in Molecular Cell Science, Innovation Center for Cell Signaling Network, Shanghai Institute of Biochemistry and Cell Biology, Chinese Academy of Sciences, Shanghai, China

4 Department of Rehabilitation, Guizhou Provincial People's Hospital, Guiyang, China

5 NHC Key Laboratory of Pulmonary Immune-related Diseases, Guizhou Provincial People's Hospital, Guiyang, China

Keywords

ATM; BCL2A1; BCL2L10; mesothelioma; UBQLN4

Correspondence

X. Zhang and Y. Nie, NHC Key Laboratory of Pulmonary Immune-related Diseases, Guizhou Provincial People's Hospital, Guiyang 550002, China
Tel: +86 851 85937194 (XYZ); +86 851 85600303 (YJN)
E-mails: zxy35762@126.com; nienyj@hotmail.com

Fang Liu, RunSang Pan, and HongYu Ding contributed equally to this work.

(Received 14 December 2020, revised 18 May 2021, accepted 9 July 2021, available online 30 August 2021)

doi:10.1002/1878-0261.13058

ATM serine/threonine kinase (ATM; previously known as ataxia-telangiectasia mutated) plays a critical role in maintaining genomic stability and regulates multiple downstream pathways, such as DNA repair, cell cycle arrest, and apoptosis. As a serine/threonine kinase, ATM has an array of downstream phosphorylation substrates, including checkpoint effector kinase 2 (CHK2). ATM inhibits cell cycle progression by phosphorylating and activating CHK2, which plays an important role in the formation and development of tumors and participates in DNA repair responses after double-stranded DNA breaks. In this study, we used a recently developed mammalian functional genetic screening system to explore a series of ATM substrates and their role in DNA damage to enhance our understanding of the DNA damage response. Ubiquitin 4 (UBQLN4), which belongs to the ubiquitin family characterized by its ubiquitin-like (UBL) and ubiquitin-associated (UBA) domains, was identified as a new substrate for ATM. UBQLN4 is involved in various intracellular processes, such as autophagosome maturation, p21 regulation, and motor axon morphogenesis. However, the biological function of UBQLN4 remains to be elucidated. In this study, we not only identified UBQLN4 as a substrate for ATM, but also found that UBQLN4 interacts with and stabilizes the anti-apoptotic proteins Bcl-2-related protein A1 (BCL2A1) and Bcl-2-like protein 10 (BCL2L10) and prevents mesothelioma cell apoptosis in response to DNA damage. These findings expand our understanding of the role of UBQLN4 in mesothelioma and provide new insights into potential mesothelioma treatments targeting substrates for ATM.

Abbreviations

53BP1, p53-binding protein 1; ATM, ataxia-telangiectasia mutation; BAP1, BRCA1-associated protein 1 gene; BCL2A1, Bcl-2-related protein A1; BCL2L10, Bcl-2-like protein 10; BRCA1, breast cancer type 1; CHK2, checkpoint effector checkpoint kinase 2; CISP, cisplatin; COX IV, cytochrome c oxidase subunit 4; CPT, camptothecin; cyto c, cytochrome c; DOX, doxorubicin; DSB, DNA double-stranded break; MDM2, murine double minute 2; MTX, methotrexate; NBS1, Nijmegen breakage syndrome protein 1; NSCLC, non-small-cell lung cancer; SMC1, structure of chromosome protein 1; TRIP12, thyroid receptor-interacting protein 12; UBA, ubiquitin associated; UBL, ubiquitin-like; UBQLN4, ubiquitin 4.

1. Introduction

Maintaining genomic stability is crucial to all living organisms [1]. As a pivotal regulator of DNA damage response, ataxia-telangiectasia mutation (ATM) kinase through checkpoint effector checkpoint kinase 2 (CHK2) pathway plays an important role in DNA damage, cell metabolism [2], and the cell cycle [3,4]. ATM also maintains the structure of chromosome protein 1 (SMC1) [5], promoting DNA repair through activation of other DNA repair proteins such as p53-binding protein 1 (53BP1) [6] and breast cancer type 1 (BRCA1) [7]. If the genome is damaged beyond repair, ATM induces programmed cell death by targeting histone H2AX [8], checkpoint protein 1 (MDC1) [9], Nijmegen breakage syndrome protein 1 (NBS1) [10], CHK2 [11], p53 [12], and murine double minute 2 (MDM2) [13]. Due to its multifaceted role in the DNA damage response, ATM dysfunction leads to several human diseases, such as breast cancer BRCA1/2 mutation-related breast cancer [14] and p53 mutation-related non-small-cell lung cancer (NSCLC) [15].

ATM phosphorylates an array of downstream substrates that play essential roles in DNA damage response. A comprehensive understanding of the interplay between these substrates in the DNA damage response is required to clarify the mechanism of DNA double-stranded break (DSB) repair and will also provide new targets for the treatment of tumors. An array of ATM/ATR substrates and unique SQ/TQ phosphorylation domains has been identified using proteomic approaches [13,16,17]. DNA damage response substrate-enriched domains including BRCT [18] and FHA [19] and histone interaction domains including TUDOR, CHROMO, and BROMO [20,21] were also identified as substrates for ATM.

In this study, we screened a library of potential ATM substrates using a recently developed mammalian functional genetic screening system based on the use of GFP-tagged shRNAs that were employed previously to explore the effect of drug sensitivity induced by specific gene knockdown on mouse E μ -Myc p19^{Arf}^{-/-} lymphoma cells [22]. Using this approach, we identified many substrates for ATM, some of which were previously validated for DNA damage, such as UBR5, thyroid receptor-interacting protein 12 (TRIP12) [23], lens epithelium-derived growth factor p75 splice variant LEGDF [24], and BRCA1-associated protein 1 gene (BAP1) [25]. This result confirmed the validity of this screening system for the identification of potential new ATM targets, and ubiquitin 4 (UBQLN4) was identified as a potential new substrate for ATM.

UBQLN4 is a member of the ubiquitin family characterized by the presence of ubiquitin-like (UBL) and ubiquitin-associated (UBA) domains. A previous study demonstrates that UBQLN4 interacts with ubiquitinated proteins and the proteasome via its UBA and UBL domains, respectively [26]. The ubiquitinated protein is then transported to the proteasome for degradation. Furthermore, recently studies suggested that UBQLN4 participates in the maturation of autophagosome regulation of p21 [27] and motor axon morphogenesis [28]. All these studies indicated that UBQLN4 plays an important role in variety cellular processes and may be a new target of precision therapy. However, the biological function of UBQLN4 in most tumors is still unclear. In this study, we not only identified UBQLN4 as new substrate for ATM, but also verified Ser318 as a major phosphorylation site following DNA damage. In a normal cell, pro- and anti-apoptotic signals work together to maintain a balance between the life and death of the cell [29]. Our further study demonstrated that UBQLN4 acts as an anti-apoptotic factor, which interacts with and stabilizes the anti-apoptotic proteins BCL2A1 and BCL2L10, and regulates mesothelioma cell apoptosis in response to DNA damage. These findings expand our understanding of the role of UBQLN4 in mesothelioma and provide a new insight into mesothelioma treatment by targeting ATM substrates.

2. Materials and Methods

2.1. Cell culture and transfection

E μ -Myc p19^{Arf}^{-/-} cell was kindly provided by Prof. Hai Jiang (Shanghai Institute of Biochemistry and Cell Biology). HEK293T, NCI-H2452, and U2OS cell lines were purchased from the Chinese Academy of Sciences cell bank (Shanghai, China). B-cell culture medium (45% Iscove's modified Dulbecco medium and 45% Dulbecco's modified Eagle's medium (DMEM) supplemented with 5 μ M β -mercaptoethanol, 10% fetal bovine serum, and L-glutamic acid) was used to culture E μ -Myc p19^{Arf}^{-/-} cells. RPMI-1640 (Gibco, Grant Island, NY, USA) containing 10% (v/v) fetal bovine serum (FBS, Biocrom, London, UK) was used to culture NCI-H2452 cells. DMEM (Gibco) containing 10% (v/v) FBS, 100 U·mL⁻¹ penicillin, and 100 μ g·mL⁻¹ streptomycin (Gibco) was used to culture HEK293T and U2OS cell lines. Polyethylenimine (Sigma, St. Louis, MO, USA) was used to transfect HEK293T cells, while U2OS cells were transfected using Lipofectamine 2000

(Invitrogen, Life Technologies, Carlsbad, CA, USA) according to the manufacturer's instructions.

2.2. Plasmid constructs

Flag-UBQLN4, HA-BCL2A1, and HA-BCL2L10 were cloned into the pCDNA3.0 vector for transiently transient transfection. BCL2A1 and BCL2L10 were cloned into pmCherry-C1 vector, and UBQLN4 was cloned into the peGFP-C1 vector for fluorescence colocalization experiments. The shRNA sequences were cloned into the lentiviral PLKO.1 vector for the ablation of UBQLN4. All restriction enzymes and ligases were purchased from NEB, and cloning was performed according to standard methods. shUBQLN4-1 : TGC TGTTGACAGTGAGCGCCACCACTTTTGAAT CTTTAATAGTGAAGCCACAGATGTATTAAGA TTGCAAAGTGGTGTTCCTACTGCCTCGGA; shUBQLN4-2 : TGCTGTTGACAGTGAGCGACCC AGAGGAAATTCGTGTGAATAGTGAAGCCACA GATGTATTCACACGAATTCCTCTGGGCTGCC TACTGCCTCGGA; shBCL2A1 : GCCAGAACAC TATTCAACCAATCAAGAGTTGGTTGAATAGTG TTCTGGCTTTTTT; shBCL2L10: GGCTTTTCTGT CATGCTTGTTC AAGAGAACAAGCATGACAGA AAAGCCTTTTT.

2.3. GFP-based cell survival competition

E μ -Myc p19^{Arf}^{-/-} cells were infected with a retrovirus expressing shRNA targeting a tumor suppressor gene and simultaneous expression of GFP. The infection efficiency of the virus was estimated to be between 20% and 40% based on the proportion of GFP-positive cells. The cells were plated into 48-well plates (10⁶ cells·well⁻¹) and treated with different drugs at a lethal dose in the range of 80% and 90%. Half of the cells were removed from each experimental group every 24 h, and fresh medium was added. After 72 h, the viability of the drug-treated and untreated cells was determined by flow cytometric analysis of propidium iodide (PI)-labeled cells. The tolerance index to the relevant drug was then calculated. Cells in the untreated group, only 250 000 cells were plated, and 75% of the medium was replaced at every 24 h to avoid excessive growth of cells.

2.4. Calculation of drug resistance or sensitivity

The formula used to calculate drug resistance or sensitivity has been described previously [21]. We introduced the concept of the relative resistance index (RI) to better describe the drug sensitivity change caused by gene knockdown. The value of RI is defined as Y,

where Y indicates that after treatment a mixture of GFP-positive and GFP-negative cells, the viability of infected (knockout) cells is changed Y-fold in comparison with that of uninfected cells. For example, if one of the F-uninfected cells survives after drug treatment, then Y cells survive after drug treatment in the F-infected cells. If we define the total number cells (infected and uninfected) as T, and the proportion of GFP-positive untreated cells as P1, the number of surviving cells that are not infected with the virus (F-un) after drug treatment is F-un = T × (1-P1) × 1/F, and the number of surviving cells that are infected with the virus (F-in) is F-in = T × P1 × Y/F. Therefore, we can calculate the proportion of GFP-positive cells in the surviving and drug-treated population (P2) as P2 = (F-in)/(F-un + F-in). Therefore, Y = (P2-P1 × P2)/(P1-P1 × P2), using this equation to calculate RI values for each shRNA-drug pair.

2.5. Cell cycle analyses

3 × 10⁵ NCI-H2452 cells were plated into 12-well plates, cultured overnight, and treated with 1 μM of camptothecin for 8 h, and then, the cells were collected and fixed overnight with 70% ethanol. Cells were then treated with 0.2% Triton X-100, 100 μg·mL⁻¹ RNase A, and 50 μg·mL⁻¹ PI for 40 min and analyzed by flow cytometry.

2.6. Apoptosis analyses

3 × 10⁵ NCI-H2452 cells were plated into 12-well plates, and the related plasmids were overexpressed after overnight culture and treated with CPT. Cell apoptosis was evaluated by flow cytometric analysis of Annexin V staining using a 633 Apoptosis Detection Kit (Dojindo, AD11, Kyushu, Japan) according to the manufacturer's instructions.

2.7. Colony formation assays

2 × 10³ NCI-H2452 cells were seeded into 6-well plates, and cells were treated with 0.2 μM, 0.5 μM, or 1 μM of camptothecin 24 h later. After another 24 h, the drug was removed and replaced with fresh medium and continued cultured at 37 °C with 5% CO₂ for 10 days. Then, the cells were fixed with 4% paraformaldehyde, stained with 0.1% crystal violet for 30 min, and washed three times with PBS before being photographed.

2.8. Cell proliferation assays

NCI-H2452 cells stably transfected with UBQLN4 shRNAs were plated in 96-well plates (5 × 10³ cells·well⁻¹

in triplicate) and treated with 4 μM , 2 μM , 1 μM , 0.5 μM , 0.25 μM , 0.125 μM , 0.0625 μM , 0.03125 μM , 0.015625 μM , or 0.007813 μM of camptothecin for 24 h. After 72 h, the number of viable cells was measured using the CCK8 method (Bimake, B34304). Briefly, CCK8 solutions were added, and the plates were incubated at 37 °C for 1 to 4 h, and then, the absorbance NCI-H2452 cells were determined using a spectrophotometric plate reader (Thermo Fisher Scientific, Waltham, MA, USA).

2.9. Immunoprecipitation and immunoblotting

Cells expressing specific endogenous or exogenous proteins were lysed with immunoprecipitation (IP) buffer supplemented with a protease inhibitor cocktail (Bimake, B14001, Houston, TX, USA). After sonication, the cell debris was removed by centrifugation (13 000 *g*, 10min), and the supernatant was aspirated and incubated with anti-flag affinity gels (Sigma, A2220) at 4 °C for overnight. The beads were then washed and denatured at 95 °C for 10 min in 2 × SDS/PAGE loading buffer. Proteins were separated by SDS/PAGE and transferred to PVDF membranes (Bio-Rad, 1620177, Guiyang, Guizhou, China). Membranes were then probed with anti-flag (ProteinTech, 20543-1-AP, 1 : 1000, Guiyang, Guizhou, China) or anti-HA (Sigma, H6908, 1 : 1000, St. Louis, MO, USA) antibodies. Secondary antibodies were labeled with HRP, and the signals were visualized using a Tanon 5200 Imaging System (Tanon, Shanghai, China).

Cells expressing the specific gene were lysed with 1 × SDS/PAGE loading buffer, denatured at 95 °C for 10 min, and subjected immunoblot analysis as described above. Detection was performed with the following antibodies : anti-UBQLN4 (Santa Cruz, sc-136560, 1 : 1000), anti-pSQ/TQ (CST, 6966, 1 : 1000), anti-BCL2A1 (ABclonal, A0134, 1 : 500), anti-BCL2L10 (ProteinTech, 18114-1-AP, 1 : 500), antitubulin (ProteinTech, 66031-1-Ig, 1 : 1000), anticytocrome c (CST, 119405, 1 : 1000), anti-COXIV (ProteinTech, 11242-1-AP, 1 : 1000).

2.10. Immunofluorescence analysis

2 × 10⁵ U2OS cells were transfected with peGFP-UBQLN4 and pmCherry-BCL2A1, or pmCherry-BCL2L10 for 48 h, and then fixed with 4% paraformaldehyde. Cells were treated with 0.5% Triton X-100 for 10 min at room temperature, and the nuclei were stained with DAPI for 5min. Image acquisition was performed with the Leica SP8, using identical confocal scan settings for each group.

2.11. Lentivirus production and infection

6 × 10⁵ HEK293T cells were seeded in 6-well plates and co-infected with pLKO.1-shRNAs and psPAX2, pMD2.G. Cultivated at 37 °C supplemented with 5% CO₂ for 72 h, then virus was harvested in 4 mL DMEM and used to infect NCI-H2452 or 293T cells. After 24 h infection, successfully infected cells were screened with puromycin for 48–72 h.

2.12. Assay for cytochrome c release from mitochondria

Mitochondria-free cytosol was prepared as previously described [30]. Briefly, 24 h after transfection and another 8 h treatment with CPT (1 μM), NCI-H2452 cells were collected and washed twice with ice-cold PBS, suspended in 100 μL extraction buffer (50 mM PIPES-KOH, pH 7.4, 200 mM mannitol, 70 mM sucrose, 50 mM KCl, 5 mM EGTA, 2 mM MgCl₂, 1 mM dithiothreitol, and protease inhibitors), and incubated on ice for 30 min. Cells were lysed by Dounce homogenization, and homogenates were centrifuged at 100 000 *g* for 15 min at 4 °C. Supernatants were harvested and analyzed by western blotting.

2.13. Immunohistochemistry (IHC) analysis of human tumor tissue array

Human mesothelioma tissue microarrays (purchased from Xi'an Elina Biotechnology Company) containing 30 mesothelioma cancer tissues and 10 adjacent normal tissues were analyzed by IHC using the VECTASTAIN ABC kit (Vector Laboratories, Burlingame, CA, USA). Rabbit primary antibodies for specific detection of UBQLN4 (ab106443, 1 : 300), BCL2A1 (ab45414, 1 : 200), and BCL2L10 (ab96625, 1 : 200) were purchased from Abcam. Sections were counterstained with hematoxylin and developed with diaminobenzidine. Immunohistochemical images were captured digitally. The expression of UBQLN4, BCL2A1, and BCL2L10 was measured by determining the integrated optical density sum of each photograph using IMAGE-PRO PLUS 5.1 software (Diagnostic Instruments, Sydney, Australia). The quantification of each sample was performed in 10 random fields (× 400) per case by two independent observers who were blinded to the clinical data. The study methodologies were approved by Guizhou University ethics committee.

2.14. Statistical analysis

All data were expressed as mean ± SEM unless stated otherwise. Student's unpaired two-tailed *t*-test (95%

confidence interval) was used to analyze data involving direct comparison of experimental and control groups. *P*-values < 0.05 were considered to indicate statistical significance.

3. Results

3.1. Systematic analysis of ATM substrates by functional genetic screening

We previously developed a functional genetic platform for the detection of genetic perturbations and altered drug sensitivities [22]. Briefly, a retrovirus encoding shRNA targeting a tumor suppressor gene and GFP were used to infect the E μ -Myc p19^{Arf}^{-/-} cell line, which was then treated with DNA damaging drugs. If oncogene deletion renders cells more resistant to DNA damaging drugs, the proportion of GFP-positive cells will increase. The platform was previously validated as a tool to study gene function and drug mechanisms [31,32]. In this study, we used the platform to identify potential ATM substrates in response to drug-induced DNA damage. Briefly, we selected a total of 52 cellular targets as potential candidates for ATM substrates based on previous publications and relevant databases containing important DNA repair domains (BRCT/FHA/SMC), or DNA or histone interaction domains (Tudor, Chromo, and Bromo) and mutated genes in cancer cell lines (Fig. 1A and Table S1). For each candidate, at least two independent shRNAs (Table S2) were pooled and used in the assay to limit the impact of off-target effects. GFP-encoded retroviruses that expressed these shRNAs were used to infect mouse E μ -Myc p19^{Arf}^{-/-} lymphoma cells to knock down the expression of target genes. If the depletion of a specific gene increases the proportion of GFP-positive cells in response to the drugs (Table S3), this gene is considered as a candidate for the DNA damage response. A reduction in GFP signal corresponds to drug sensitization, whereas increased GFP expression is interpreted as drug resistance (Fig. 1B).

For the control retrovirus vector did not alter drug sensitivity in our study, thus any changes in drug sensitivity were attributed to shRNA-mediated gene silencing (Fig. 1C). Many advantages of this method make it beneficial for gene function studies of responses to DNA damage. E μ -Myc p19^{Arf}^{-/-} cells have a relatively simple genetic landscape, and the data are highly reproducible since each sensitivity reading represents the results of tens of thousands of tumor suppressor-deficient cells and collective survival of proficient cells. Finally, GFP-negative candidate-

proficient cells serve as internal controls, which helps circumvent and normalizes sample-to-sample variability due to inaccurate cell passaging, cell seeding, different serum batches, medium evaporation, and other factors that could impact the consistency of the MTT assays.

As a proof of concept, we first evaluated the correlation between known tumor suppressor genes and drug sensitivity. It is well documented that deficiency in CHK1, RAD51D, and BRCA1/2 [14,33] leads to cisplatin hypersensitivity, while CHK2 and p53 deficiency alters cisplatin resistance [34]. As expected, all five of the anticipated cisplatin sensitivity phenotypes were confirmed in our study (Fig. 1D). These results were consistent with clinical observations and validated the accuracy of our methods. After the proof-of-concept and validation studies, we then further employed this method to screen substrates for ATM in 52 candidates as described.

3.2. Confirmation of UBQLN4 as an ATM substrate that alters the cellular response to DNA damaging agents

The functional genetic screening results were analyzed using a previously developed calculation method [22] as described in the Experimental Procedures section. The best signal obtained from three shRNAs of the 52 potential ATM substrates screened is shown in Fig. 1E and Table S1. As a potential ATM substrate, UBQLN4 was chosen for further study. Our study demonstrated that the silencing of UBQLN4 resulting in significantly enhanced sensitivity to several DNA damaging agents (Fig. 2A–B). Endogenous UBQLN4 was phosphorylated in response to cisplatin, which was reduced by the ATM inhibitor KU55933, suggesting that the pSQ/TQ sites of UBQLN4 are ATM targets (Fig. 2C). Examine the full wild-type UBQLN4 protein sequence to further map the specific residues phosphorylated revealed the serine residue at position 318 as the most likely candidate. Indeed, the mutated UBQLN4 (S318A) was no longer phosphorylated in response to DNA damage (Fig. 2D). These results confirmed that UBQLN4 is a new substrate for ATM, and Ser318 is a major phosphorylation site in response to DNA damage.

3.3. UBQLN4 is highly expressed in mesothelioma

According to the data from TCGA database, UBQLN4 is amplified in many cancers, the red part represents amplification, the green part represents

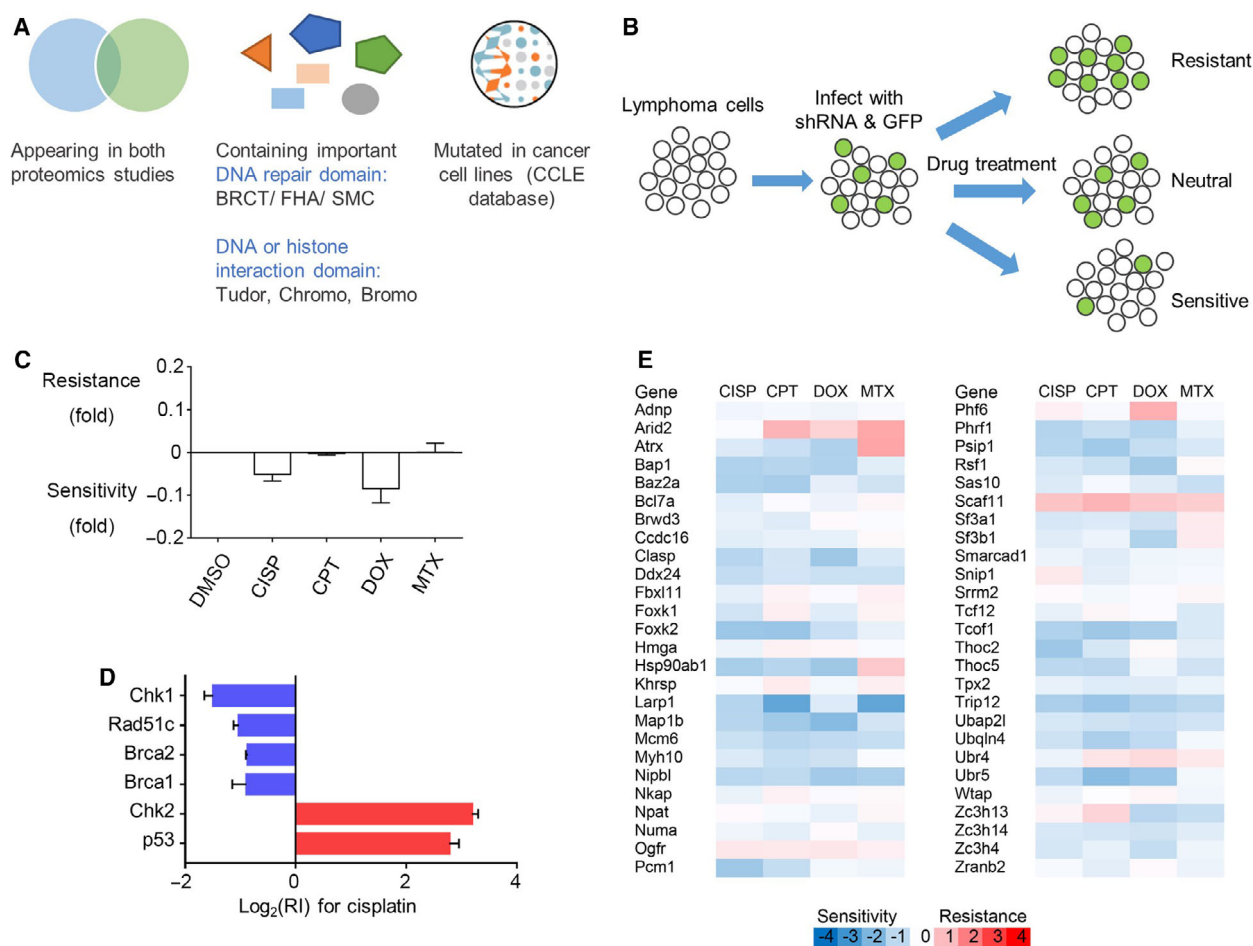


Fig. 1. Identification of potential ATM substrate by functional screening. (A) Diagram of the ATM candidates. The potential ATM substrates were chosen from the overlap gene, which contains important DNA repair domains: BRCT/FHA/SMC, or DNA or histone interaction domains: Tudor, Chromo, Bromo, and mutated genes in cancer cell lines. (B) Cell survival assay based on GFP fluorescence. E μ -Myc p19^{Arf}^{-/-} lymphoma cells were stably transduced with a recombinant retrovirus expressing shRNA and GFP. The shRNA-mediated alterations in sensitivity to a specific DNA damage reagent were manifested as a change in the number of GFP-positive cells. (C) Drug susceptibility to DNA damage drugs was detected in cells, CISP, CPT, DOX, and MTX. Values were normalized against vehicle controls. Data are presented in mean \pm SEM, $n = 3$. (D) Proof-of-concept analysis showed that the depletion of known ATM targets including CHK1 and CHK2 altered the sensitivity to cisplatin. Data are presented in mean \pm SEM, $n = 3$. (E) Heatmap summarizing how the depletion of potential ATM substrates leads to sensitivity (blue) or resistance (red) to a drug. For each gene, independent shRNAs exhibited similar resistance or sensitivity phenotypes.

mutation, and the blue part represents deletion (Fig. 3A). Survival analysis of the TCGA mesothelioma cancer database using GEPIA suggested that cancer patients with low levels of UBQLN4 survived significantly longer than those with high levels of UBQLN4 (Fig. 3B). In addition to the elevated gene expression, immunohistochemistry (IHC) analysis of human mesothelioma tissue arrays containing 30 mesothelioma tissues and 10 adjacent normal tissues showed that UBQLN4 expression was also significantly increased at the protein level. The detailed clinical data for these patients are shown in Table S4, and

two representative images are shown in Fig. 3C. Stronger UBQLN4 staining was observed in the mesothelioma tissues compared with that of adjacent tissues (Fig. 3D). Collectively, these data suggested that UBQLN4 upregulation may be associated with development or prognosis of mesotheliomas.

3.4. UBQLN4 regulates mesothelioma cell apoptosis in response to DNA damage

The colony formation and cell viability assays of human mesothelioma NCI-H2452 cells indicated that

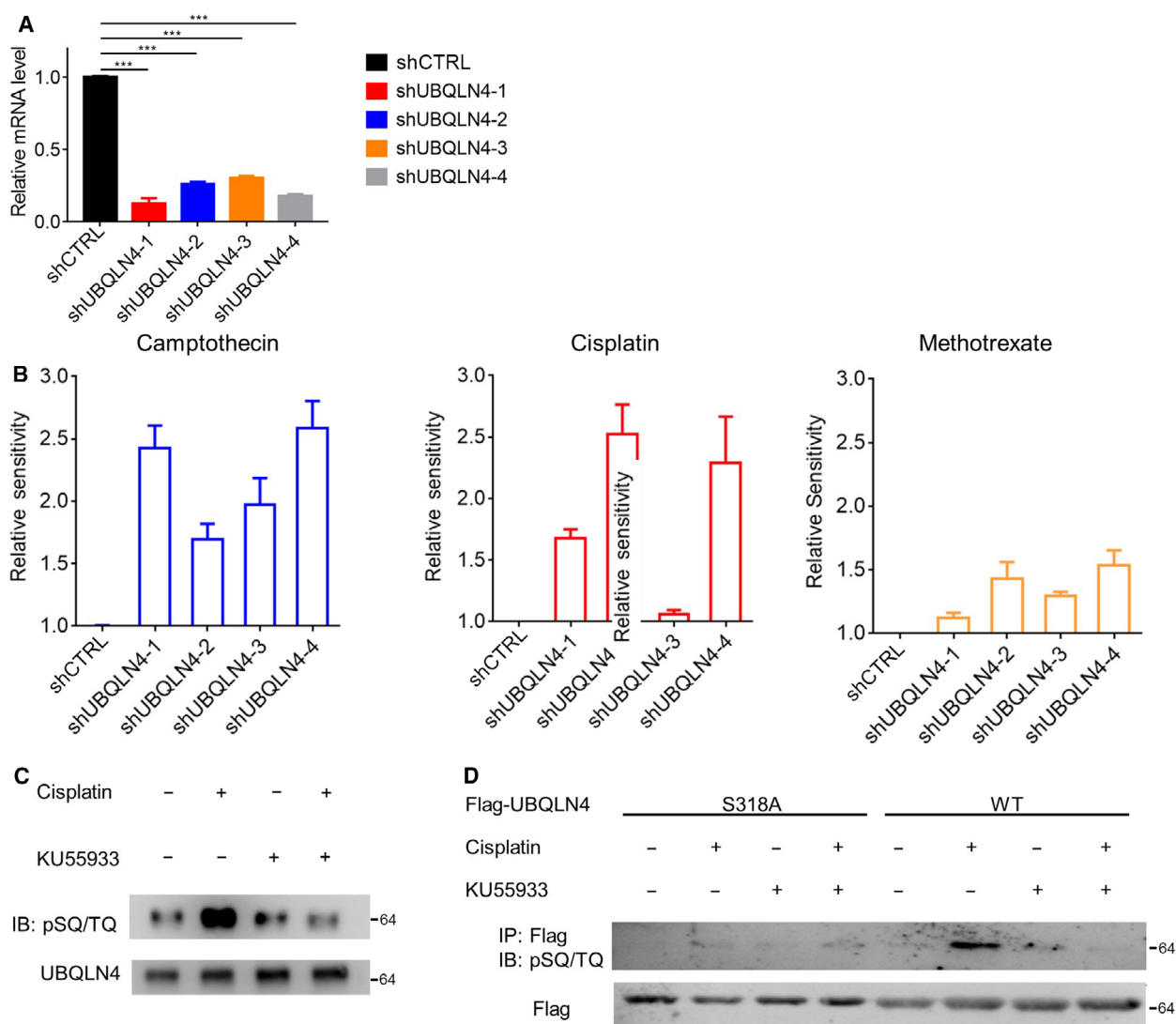


Fig. 2. UBQLN4 was identified as an ATM pathway substrate. (A) The knockdown efficiency of UBQLN4 in E μ -Myc p19^{Arf}^{-/-} cells was analyzed by qPCR. Data are presented in mean \pm SEM, $n = 3$. Significance was determined by Student's t -test. *** $P < 0.001$. (B) Effect of UBQLN4 knockdown on E μ -Myc p19^{Arf}^{-/-} cell sensitivity to DNA damage drugs (cisplatin, camptothecin, and methotrexate). Data are presented in mean \pm SEM, $n = 3$. (C) HEK293T cells were treated with cisplatin and the ATM inhibitor KU55933 for 12 h. Endogenous UBQLN4 and ATM phosphorylation substrate-specific antibodies (pSQ/TQ) were assessed, $n = 3$. (D) Wild-type UBQLN4 or its S318A mutant was overexpressed in HEK293T cells. After 12 h of treatment with cisplatin and KU55933, UBQLN4 was immunoprecipitated with flag beads and subjected to immunoblotting analysis, $n = 3$.

UBQLN4-silencing inhibited mesothelioma cell colony formation and significantly enhanced the mesothelioma cell sensitivity to DNA damaging drugs (Fig. 4A–B). Subsequently, Annexin V/PI staining assays showed a higher rate of apoptosis in UBQLN4-deficient cells than that in control cells, suggesting that UBQLN4 regulates apoptosis in response to DNA damage (Fig. 4C–E). Furthermore, compared with UBQLN4-S318A, overexpression wild-type UBQLN4 significantly enhanced drug

resistance to CPT treatment (Fig. 4F). The apoptosis induced by knockdown UBQLN4 could be restored by overexpression of UBQLN4-WT, while UBQLN4-S318A could not (Fig. 4G–H). Flow cytometry analysis revealed that UBQLN4 silencing had no effects on cell cycle progression (Fig. 4I–J). Taken together, our data suggest that ATM-mediated phosphorylation of UBQLN4 at Ser318 may regulate mesothelioma cell apoptosis in response to DNA damage.

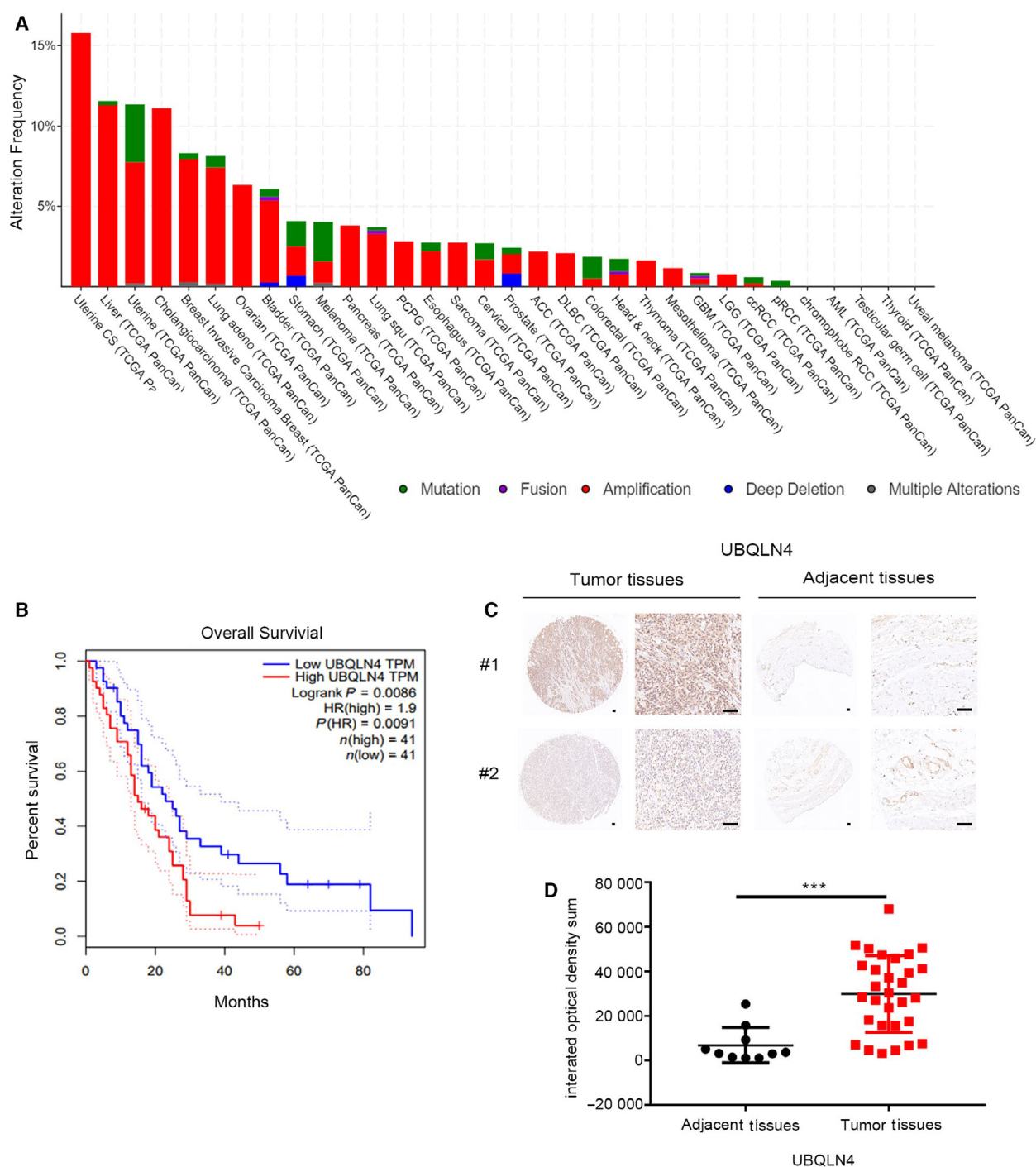


Fig. 3. UBQLN4 is overexpressed in mesothelioma. (A) The X-axis represents different tumor types, and the Y-axis represents the alteration frequency, the red part represents amplification, the green part represents mutation, and the blue part represents deletion. (B) Correlation between UBQLN4 expression in mesothelioma and survival. GEPIA program from TCGA MESO datasets was used to construct Kaplan–Meier survival curves. Blue and red curves denote low- and high-risk groups, respectively. X-axis indicates the survival in months, and the Y-axis represents the percentage survival. (C) Representative images of immunohistochemical staining of UBQLN4 in tumor tissues ($n = 30$) and adjacent tissues ($n = 10$). Scale bar, 100 μm . (D) The integrated optical density sum of UBQLN4 in tumor tissues ($n = 30$) and adjacent tissues ($n = 10$). Significance was determined by Student's *t*-test. Data are presented in mean \pm SEM, *** $P < 0.001$.

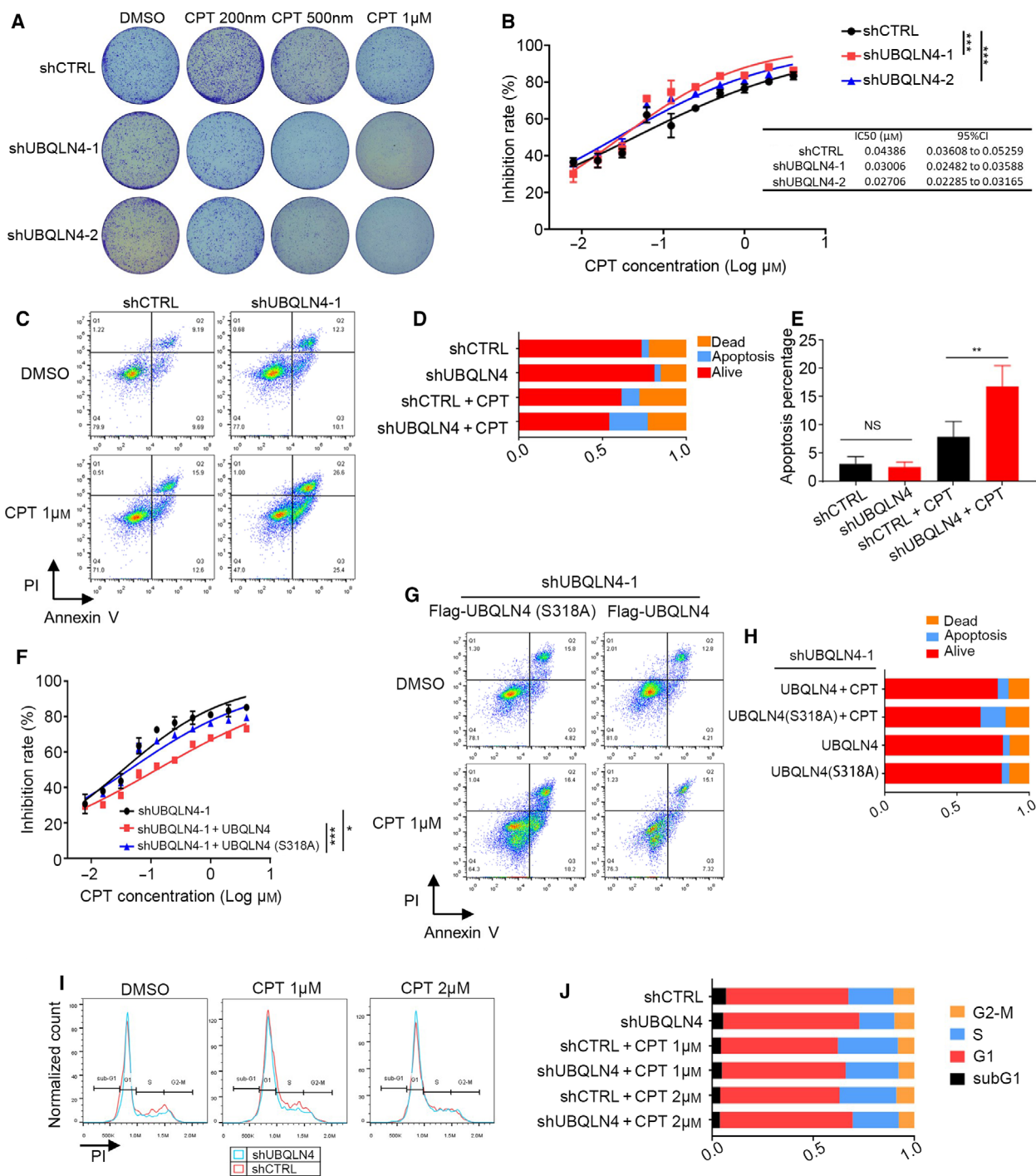


Fig. 4. UBQLN4 regulates apoptosis in response to DNA damage. (A) UBQLN4 depletion sensitizes human mesothelioma NCI-H2452 cells to DNA damaging drugs. Cell colonies were grown for 10 days after treating with CPT for 24 h, $n = 3$. (B) CCK8 assays were used to assess the viability of NCI-H2452 cells following treated with CPT for 24 h. Significance was determined by one-way ANOVA. Data are presented in mean \pm SEM, $n = 3$, $***P < 0.001$. (C–E) UBQLN4-depleted NCI-H2452 cells undergo increased levels of apoptosis in response to CPT (1 μ M, 8 h). Significance was determined by Student's t -test. Data are presented in mean \pm SEM, $n = 3$, $**P < 0.01$. (F) CCK8 assays were used to assess the viability of NCI-H2452 cells following treated with CPT for 24 h. Significance was determined by one-way ANOVA. Data are presented in mean \pm SEM, $n = 3$, $***P < 0.001$. $*P < 0.05$. (G–H) UBQLN4 or UBQLN4(S318A) were overexpressed in UBQLN4 knockdown NCI-H2452 cells, and levels of the apoptosis were evaluated by flow cytometric analysis in response to CPT (1 μ M, 8 h). Data are presented in mean \pm SEM, $n = 3$. (I–J) UBQLN4 silencing does not alter the cell cycle status of NCI-H2452 cells treated with CPT (1 μ M, 8 h). Data are presented in mean \pm SEM, $n = 3$.

3.5. UBQLN4 interacts with and stabilizes the anti-apoptotic proteins BCL2A1 and BCL2L10

We next explored the role of UBQLN4 during apoptosis induction. UBQLN1, which is similar to UBQLN4,

has been shown to interact with one of the BCL2 family members, BCL2L10, regulating its ubiquitination, intracellular localization, and stability. Therefore, we hypothesized that UBQLN4 might also interact with the members of BCL2 family. To test this hypothesis,

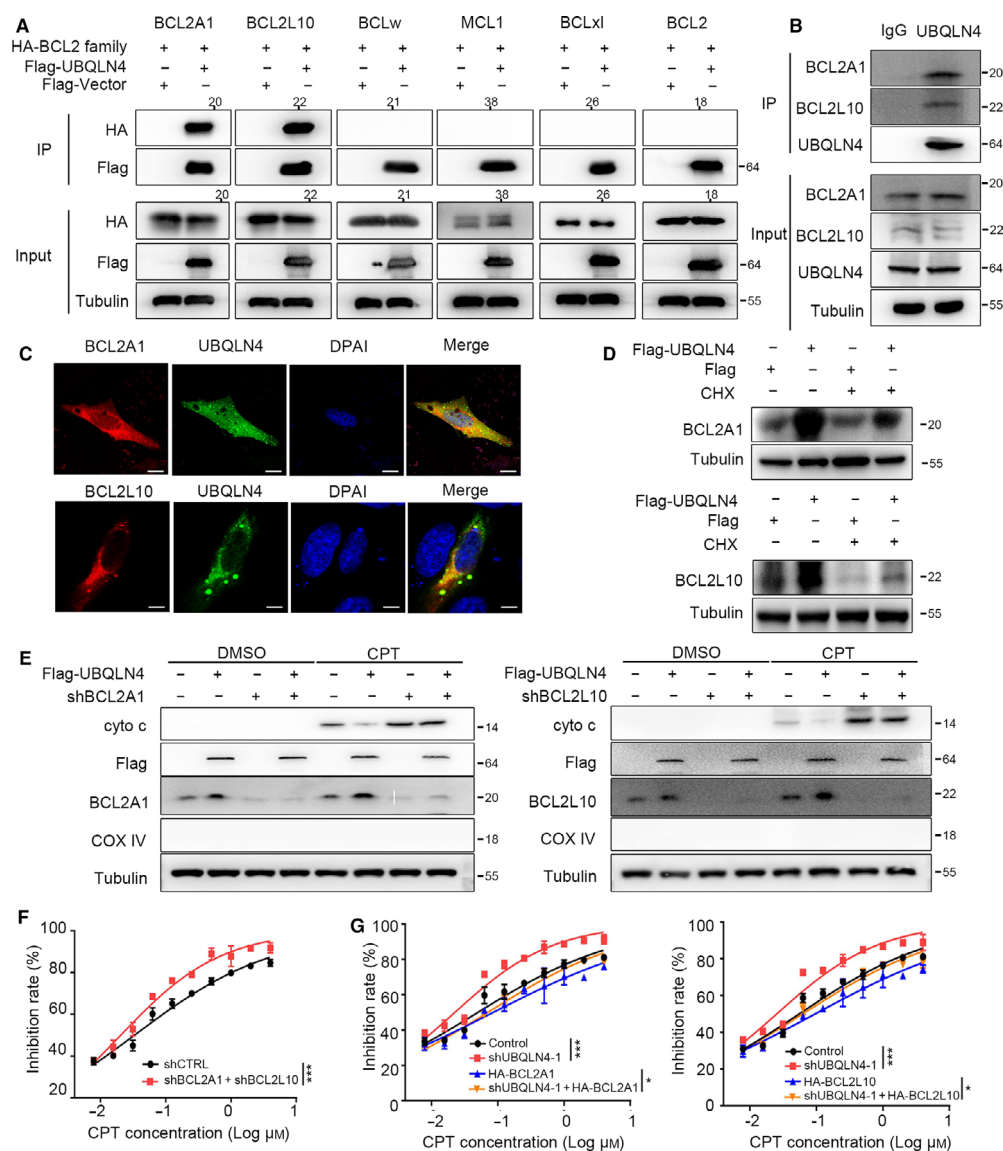


Fig. 5. UBQLN4 interacts with and stabilizes BCL2A1/BCL2L10. (A) Co-immunoprecipitation assays showing the interaction between ectopic UBQLN4 and BCL2A1, or BCL2L10, $n = 3$. (B) Co-immunoprecipitation assay showed that endogenous UBQLN4 and BCL2A1 or BCL2L10 formed a complex, $n = 3$. (C) UBQLN4 colocalizes with BCL2A1 and BCL2L10. U2OS cells were cotransfected with pEGFP-UBQLN4 and BCL2A1-RFP, or BCL2L10-RFP. Scale bar, 10 μm , $n = 3$. (D) UBQLN4 overexpression stabilizes BCL2A1 and BCL2L10. HEK293T cells were transfected with empty vectors or vectors expressing UBQLN4, and treated with CHX (100 $\mu\text{g}\cdot\text{mL}^{-1}$) for 12 h, $n = 3$. (E) The cyto3 was upregulated in NCI-H2452 cells with BCL2A1 or BCL2L10 knockdown. After cell isolation, mitochondria-free cytosol was collected for immunoblot with indicated antibodies, $n = 3$. (F) BCL2A1 and BCL2L10 were knocked down in mesothelioma cells and treated with CPT for 24 h. The cell viability was detected by CCK8 assay. Significance was determined by one-way ANOVA. Data are presented in mean \pm SEM. *** $P < 0.001$. (G) CCK8 assays were used to assess the viability of NCI-H2452 cells following treated with CPT for 24 h. Significance was determined by one-way ANOVA. Data are presented in mean \pm SEM, $n = 3$, *** $P < 0.001$. * $P < 0.05$.

we performed co-immunoprecipitation analysis of UBQLN4 with six BCL2 family members. Flag-tagged UBQLN4 and HA-tagged BCL2, BCL2L10, BCLxL, BCLw, MCL1, and BCL2A1 were generated and cotransfected into HEK293T cells for co-immunoprecipitation analysis. Cotransfection of UBQLN4 with individual BCL2 family members showed that UBQLN4 only interacted with BCL2A1 and BCL2L10, but not to other members of the BCL2 family (Fig. 5A). In addition, the endogenous UBQLN4 also could interact with the endogenous BCL2A1 and BCL2L10 (Fig. 5B). These interactions were further confirmed by colocalization assays using the fluorescent fusion proteins peGFP-UBQLN4, and pmCherry-BCL2A1 or pmCherry-BCL2L10 expressed in U2OS cells (Fig. 5C). Next, the mechanism of UBQLN4 regulates BCL2A1 and BCL2L10 was investigated, and we found that overexpression of UBQLN4 in 293T cells led to an increase in BCL2A1 and BCL2L10 expression, suggesting that UBQLN4 can stabilize BCL2A1 and BCL2L10 (Fig. 5D). It is reported that the BCL2 family can inhibit mitochondrial outer membrane permeability (MOMP) and play an anti-apoptotic effect [35,36]. Therefore, we further investigated the anti-apoptotic mechanisms of BCL2A1 and BCL2L10 in mesothelioma and found that UBQLN4 could prevent MOMP in mesothelioma cells with CPT treatment. Knockdown of BCL2A1 and BCL2L10 both could increase the MOMP and only partially rescue the effect of UBQLN4 treated with CPT (Fig. 5E). Besides, we found that the depletion of BCL2A1 and BCL2L10 could enhance the sensitivity to the treatment of CPT in mesothelioma cells (Fig. 5F). Furthermore, overexpression of BCL2A1 or BCL2L10 could rescue the effect of UBQLN4 depletion under the treatment of CPT (Fig. 5G). These results suggested that UBQLN4 regulates the apoptosis of cells by stabilizing BCL2A1 and BCL2L10.

3.6. BCL2A1 and BCL2L10 are highly expressed in mesothelioma which correlates with the expression of UBQLN4

Immunohistochemistry assays indicated that BCL2A1 and BCL2L10 are highly expressed in mesothelioma. As shown in Fig. 6A and Fig. 6B, much stronger staining for BCL2A1(A) or BCL2L10 (B) was observed in the tumors (left) compared with that in adjacent tissues (right). The expression of BCL2A1 and BCL2L10 was measured by determining the integrated optical density of each photograph as in Fig. 6C (BCL2A1) and Fig. 6D (BCL2L10). All three proteins, UBQLN4,

BCL2A1, and BCL2L10, were highly expressed in all cases of mesothelioma tissues. The expression of UBQLN4 with BCL2A1 and BCL2L10 showed a positive correlation (Fig. 6E and 6F).

4. Discussion

In this study, we used a recently developed mammalian functional genetic screening system to explore new ATM substrates in a total of 52 cellular targets as potential candidates. We found UBQLN4 as a new ATM substrate, which was upregulated in mesothelioma. High level of UBQLN4 led to poorer prognosis than those with low levels of UBQLN4. Mechanically, UBQLN4 regulates mesothelioma cell apoptosis in response to DNA damage by phosphorylating the site of Ser318. Furthermore, UBQLN4 interacts with BCL2A1 and BCL2L10 and enhances the drug resistance by stabilizing BCL2A1 and BCL2L10. Our results thus not only revealed lots of potential candidates for ATM but also unveiled a mechanism that a new ATM substrate UBQLN4 regulates apoptosis in mesothelioma by stabilizing BCL2A1 and BCL2L10. Taken together, our data suggest that ATM-mediated phosphorylation of UBQLN4 at Ser318 may regulate mesothelioma cell apoptosis in response to DNA damage.

Malignant mesothelioma (MM) is a rare neoplasm with poor prognosis, which arises primarily from the surface serosal cells of the pleura, peritoneum, and pericardium and has been classified histologically into three subtypes: epithelioid, sarcomatoid, and biphasic [37]. According to reports, the median survival of patients with mesothelioma is only 8.9–14 months [38,39]. There are no generally accepted guidelines for radical treatment of MM. For example, the common treatment methods such as radiotherapy and chemotherapy cannot achieve good treatment results. The finding that UBQLN4 is high expressed in mesothelioma and knockdown of UBQLN4 enhances the sensitivity to DNA damage drugs may provide a new molecular strategy for the treatment of malignant mesothelioma.

Ataxia-telangiectasia mutation (ATM) kinase, as a vital regulator of DNA damage response, plays a significant role in DNA damage, cell metabolism [2], and the cell cycle by phosphorylating an array of downstream substrates [3,4]. If the damages overweight the repair in genome, ATM could induce programmed cell death by targeting histone H2AX, MDC1, NBS1, CHK2, p53, and MDM2 [8-13]. In this study, we are the first to use new method to screen substrates for ATM, and the screening result not only accurate but also repeatable, which provides a potential molecular database and a series of new ideas for exploring ATM substrates.

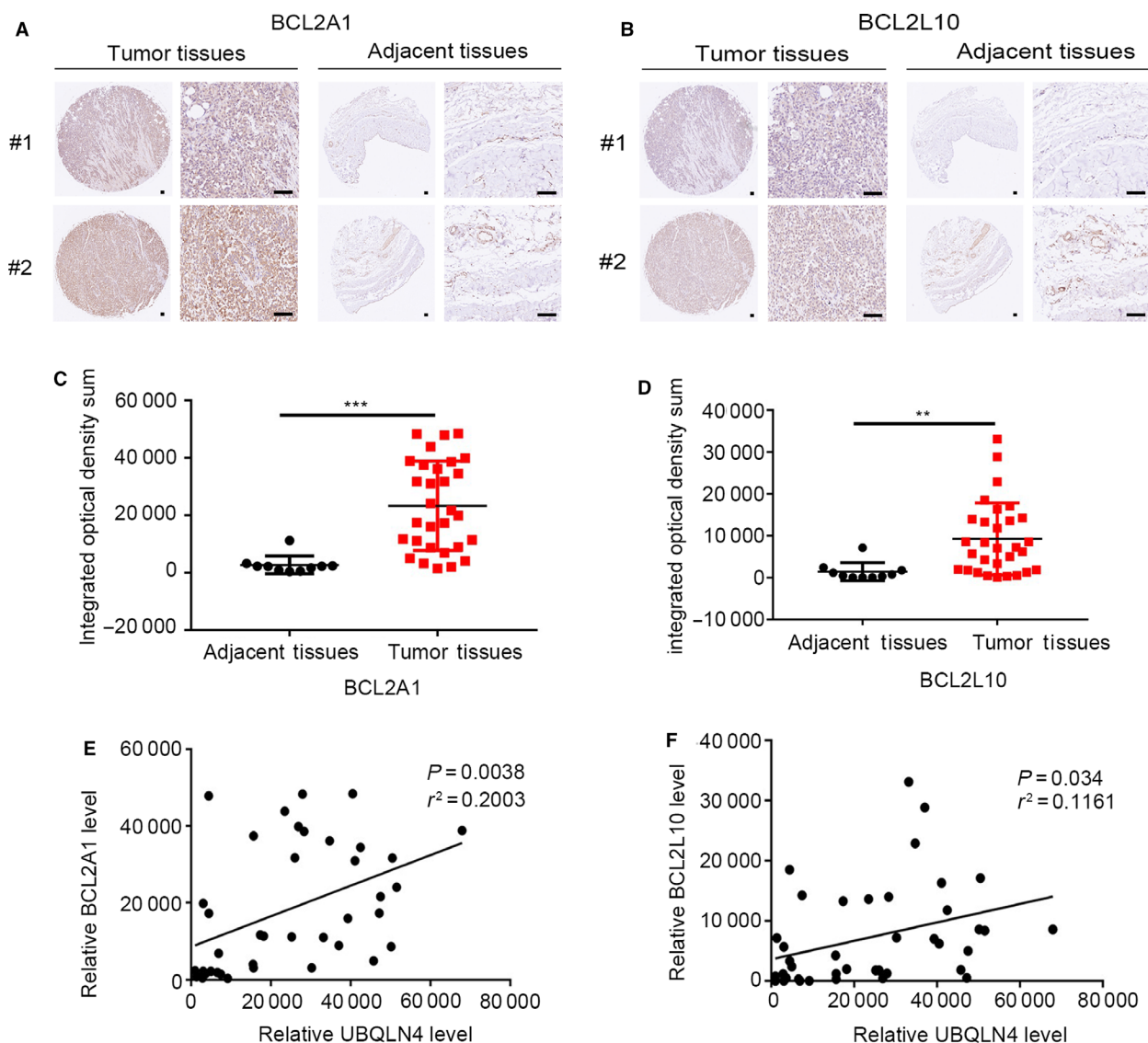


Fig. 6. BCL2A1 and BCL2L10 are highly expressed in mesothelioma, and their expressions correlate with UBQLN4 level. (A) Immunohistochemistry shows the staining of BCL2A1 in tumor tissues ($n = 30$) and its adjacent tissues ($n = 10$). Scale bar, 100 μm . (B) Immunohistochemistry shows the staining of BCL2L10 in tumor tissues ($n = 30$) and its adjacent tissues ($n = 10$). Scale bar, 100 μm . (C–D) Statistics integrated optical density sum BCL2A1 (C) and BCL2L10 (D) staining in human mesothelioma tissues. Significance was determined by Student's *t*-test. Data are presented in mean \pm SD, $**P < 0.01$, $***P < 0.001$ (E–F). A correlation between UBQLN4 and BCL2A1 (E) or BCL2L10 (F) in mesothelium tissues ($n = 40$) was identified by Pearson's *r*. $**P < 0.01$, $*P < 0.05$.

Ubiquilins (Ubqlns) is a type of cytoplasmic protein that exerts protein degradation by enhancing autophagy-mediated degradation and participating in endoplasmic reticulum-related protein degradation [40,41]. UBQLN4 is a member of the ubiquitin family that consists of five known members (ubiquitin 1, ubiquitin 2, ubiquitin 3, ubiquitin 4, and ubiquitin L) and has emerged as a candidate substrate for ATM. Recent studies have shown that UBQLN4 is involved in various intracellular processes such as autophagosome

maturation, p21 regulation [27], and motor axon morphogenesis [28]. However, the biological function of UBQLN4 in most tumors is not clear. In this study, we not only confirmed that UBQLN4 is an ATM substrate but also verified that Ser318 is a major phosphorylation site following DNA damage. Furthermore, UBQLN4 inhibits the apoptosis in mesothelioma by stabilizing BCL2A1 and BCL2L10. All of these findings increase our understanding of UBQLN4 in DNA damage. However, how UBQLN4 stabilizes BCL2A1

and BCL2L10 still needs further research and exploration. This could be a new feature and mechanism of the ubiquilin family.

5. Conclusions

Taken together, we uncover that about fifty potential substrates for ATM and clarify the mechanism that UBQLN4 inhibits the apoptosis in mesothelioma by phosphorylating the site of Ser318 and stabilizing BCL2A1 and BCL2L10. UBQLN4 may be of great therapeutic potential for targeting mesothelioma and other diseases. Other potential substrates of ATM need be further explored to clarify the network of ATM and may act as a potential therapeutic target or provide new therapeutic strategies for human diseases.

Conflict of interest

The authors declare that they have no conflict of interest.

Acknowledgments

This work was supported by the Nonprofit Central Research Institute Fund of Chinese Academy of Medical Sciences 2019PT320003, Guizhou Provincial Peoples Hospital (GZSYQCC[2015]004), Guizhou Science and Technology Immunology and Infection Platform (2018-5706), National Natural Science Foundation of China (82060308), and China Postdoctoral Science Foundation (Grant No. 2018M630480). We thank the Core Facility for Cell Biology at SIBCB and the talent base program from Guizhou Talent Office.

Peer Review

The peer review history for this article is available at <https://publons.com/publon/10.1002/1878-0261.13058>.

Data accessibility

All experimental data during this research are included in the published article and its supplementary files. The datasets and materials in this study are available on reasonable request from corresponding authors or first author.

Author contributions

FL, HYD, and LLG designed the experiments. FL, RSP, and HYD performed most of the experiments. LLG, YY, CYL, YJX, and HC performed part of the experiments. FL, RSP, and HYD prepared and wrote

the manuscript. XYZ, YJN, and RGH reviewed and edited the manuscript. All authors discussed the results and commented on the manuscript.

References

- Ciccica A & Elledge SJ (2010) The DNA damage response: making it safe to play with knives. *Mol Cell* **40**, 179–204.
- Guo Q-Q, Wang S-S, Zhang S-S, Xu H-D, Li X-M, Guan Y, Yi F, Zhou T-T, Jiang B *et al.* (2020) ATM-CHK2-Beclin 1 axis promotes autophagy to maintain ROS homeostasis under oxidative stress. *EMBO J* **39**, e103111.
- McKinnon PJ (2012) ATM and the Molecular Pathogenesis of Ataxia Telangiectasia. *Annu Rev Pathol* **7**, 303–321.
- Zhang W-Y, Feng Y-L, Guo Q-Q, Guo W-D, Xu H-D, Li X-M, Yi F, Geng N-X, Wang P-Y *et al.* (2020) SIRT1 modulates cell cycle progression by regulating CHK2 acetylation–phosphorylation. *Cell Death Differ* **27**, 482–496.
- Yazdi PT, Wang Y, Zhao S, Patel N, Lee EY-HP & Qin J (2002) SMC1 is a downstream effector in the ATM/NBS1 branch of the human S-phase checkpoint. *Genes Dev* **16**, 571–582.
- Schultz LB, Chehab NH, Malikzay A & Halazonetis TD (2000) p53 binding protein 1 (53BP1) is an early participant in the cellular response to DNA double-strand breaks. *J Cell Biol* **151**, 1381–1390.
- Li S, Ting NS, Zheng L, Chen PL, Ziv Y, Shiloh Y, Lee EY & Lee WH (2000) Functional link of BRCA1 and ataxia telangiectasia gene product in DNA damage response. *Nature* **406**, 210–215.
- Burma S, Chen BP, Murphy M, Kurimasa A & Chen DJ (2001) ATM Phosphorylates Histone H2AX in Response to DNA Double-strand Breaks. *J Biol Chem* **276**, 42462–42467.
- Goldberg M, Stucki M, Falck J, D'Amours D, Rahman D, Pappin D, Bartek J & Jackson SP (2003) MDC1 is required for the intra-S-phase DNA damage checkpoint. *Nature* **421**, 952–956.
- Lim DS, Kim ST, Xu B, Maser RS, Lin J, Petrini JH & Kastan MB (2000) ATM phosphorylates p95/nbs1 in an S-phase checkpoint pathway. *Nature* **404**, 613–617.
- Matsuoka S, Huang M & Elledge SJ (1998) Linkage of ATM to cell cycle regulation by the Chk2 protein kinase. *Science* **282**, 1893–1897.
- Hirao A, Kong Y-Y, Matsuoka S, Wakeham A, Ruland J, Yoshida H, Liu D, Elledge SJ, Mak TW *et al.* (2000) DNA Damage-induced activation of p53 by the checkpoint kinase Chk2. *Science* **287**, 1824–1827.
- Bensimon A, Schmidt A, Ziv Y, Elkon R, Wang S-Y, Chen D-J, Ebersold R & Shiloh Y (2010) ATM-dependent and -independent dynamics of the nuclear phosphoproteome after DNA damage. *Sci Signal* **3**, rs3.

- 14 Tan DSP, Rothermundt C, Thomas K, Bancroft E, Eeles R, Shanley S, Jones AA, Norman A, Kaye SB *et al.* (2008) “BRCAness” syndrome in ovarian cancer: a case-control study describing the clinical features and outcome of patients with epithelial ovarian cancer associated with BRCA1 and BRCA2 mutations. *J Clin Oncol* **26**, 5530–5536.
- 15 Chen Y, Chen G, Li J, Huang Y-Y, Li Y, Lin J, Chen L-Z, Lu J-P, Wang Y-Q *et al.* (2019) Association of tumor protein p53 and ataxia-telangiectasia mutated comutation with response to immune checkpoint inhibitors and mortality in patients with non-small cell lung cancer. *JAMA Netw Open* **2**, e1911895.
- 16 Matsuoka S, Ballif BA, Smogorzewska A, 3rd ERM, Hurov KE, Luo J, Bakalarski CE, Zhao ZM, Solimini N *et al.* (2007) ATM and ATR substrate analysis reveals extensive protein networks responsive to DNA damage. *Science* **316**, 1160–1166.
- 17 Beli P, Lukashchuk N, Wagner S, Weinert BT, Olsen JV, Baskcomb L, Mann M, Jackson SP, Choudhary C *et al.* (2012) Proteomic investigations reveal a role for RNA processing factor THRAP3 in the DNA damage response. *Mol Cell* **46**, 212–225.
- 18 Williams RS, Lee MS, Hau DD & Glover JNM (2004) Structural basis of phosphopeptide recognition by the BRCT domain of BRCA1. *Nat Struct Mol Biol* **11**, 519–525.
- 19 Matsuura S, Kobayashi J, Tauchi H & Komatsu K (2004) Nijmegen breakage syndrome and DNA double strand break repair by NBS1 complex. *Adv Biophys* **38**, 65–80.
- 20 Botuyan MV, Lee J, Ward IM, Kim J-E, Thompson JR, Chen JJ & Mer G (2006) Structural basis for the methylation state-specific recognition of histone H4–K20 by 53BP1 and Crb2 in DNA Repair. *Cell* **127**, 1361–1373.
- 21 Kim J, Daniel J, Espejo A, Lake A, Krishna M, Xia L, Zhang Y & Bedford M T (2006) Tudor, MBT and chromo domains gauge the degree of lysine methylation. *EMBO Rep* **7**, 397–403.
- 22 Jiang H, Pritchard JR, Williams RT, Lauffenburger DA & Hemann MT (2011) A mammalian functional-genetic approach to characterizing cancer therapeutics. *Nat Chem Biol* **7**, 92–100.
- 23 Gudjonsson T, Altmeyer M, Savic V, Toledo L, Dinant C, Grøfte M, Bartkova J, Poulsen M, Oka Y *et al.* (2012) TRIP12 and UBR5 suppress spreading of chromatin ubiquitylation at damaged chromosomes. *Cell* **150**, 697–709.
- 24 Daugaard M, Baude A, Fugger K, Povlsen LK, Beck H, Sørensen CS, Petersen NH, Sorensen NH, Lukas C *et al.* (2012) LEDGF (p75) promotes DNA-end resection and homologous recombination. *Nat Struct Mol Biol* **19**, 803–810.
- 25 Yu H, Pak H, Hammond-Martel I, Ghram M, Rodrigue A, Daou S, Barbour H, Corbeil L, Hébert J *et al.* (2014) Tumor suppressor and deubiquitinase BAP1 promotes DNA double-strand break repair. *PNAS* **111**, 285–290.
- 26 Su V & Lau AF (2009) Ubiquitin-like and ubiquitin-associated domain proteins: significance in proteasomal degradation. *Cell Mol Life Sci* **66**, 2819–2833.
- 27 Huang S, Li Y, Yuan X, Zhao M, Wang J, Li Y, Li Y, Lin H, Zhang Q *et al.* (2019) The UbL-UBA Ubiquilin4 protein functions as a tumor suppressor in gastric cancer by p53-dependent and p53-independent regulation of p21. *Cell Death Differ* **26**, 516–530.
- 28 Edens BM, Yan J, Miller N, Deng H-X, Siddique T & Ma YC (2017) A novel ALS-associated variant in UBQLN4 regulates motor axon morphogenesis. *Elife* **6**, e25453.
- 29 Levy JMM & Thorburn A (2020) Autophagy in cancer: moving from understanding mechanism to improving therapy responses in patients. *Cell Death Differ* **27**, 843–857.
- 30 Essmann F, Bantel H, Totzke G, Engels IH, Sinha B, Osthoff K & Jänicke RU (2003) Staphylococcus aureus α -toxin-induced cell death: predominant necrosis despite apoptotic caspase activation. *Cell Death Differ* **10**, 1260–1272.
- 31 Pritchard JR, Bruno PM, Gilbert LA, Capron KL, Lauffenburger DA & Hemann MT (2013) Defining principles of combination drug mechanisms of action. *Proc Natl Acad Sci* **110**, E170–E179.
- 32 Bruno PM, Liu Y, Park GY, Murai J, Koch CE, Eisen TJ, Pritchard JR, Pommier Y, Lippard SJ & Hemann MT (2017) A subset of platinum-containing chemotherapeutic agents kills cells by inducing ribosome biogenesis stress. *Nat Med* **23**, 461–471.
- 33 Farmer H, McCabe N, Lord CJ, Tutt AN, Johnson DA, Richardson TB, Santarosa M, Dillon KJ, Hickson I *et al.* (2005) Targeting the DNA repair defect in BRCA mutant cells as a therapeutic strategy. *Nature* **434**, 917–921.
- 34 Jiang H, Wu J, He C, Yang W & Li H (2009) Tumor suppressor protein C53 antagonizes checkpoint kinases to promote cyclin-dependent kinase 1 activation. *Cell Res* **19**, 458–468.
- 35 Deng J (2017) How to unleash mitochondrial apoptotic blockades to kill cancers? *Acta Pharm Sin B* **7**, 18–26.
- 36 Kalkavan H & Green DR (2018) MOMP, cell suicide as a BCL-2 family business. *Cell Death Differ* **25**, 46–55.
- 37 Husain AN, Colby TV, Ordóñez NG, Allen TC, Attanoos RL, Beasley MB, Butnor KJ, Chirieac LR, Churg AM *et al.* (2017) Guidelines for pathologic diagnosis of malignant mesothelioma 2017 update of the consensus statement from the international mesothelioma interest group. *Arch Pathol Lab Med* **142**, 89–108.

- 38 Edwards J, Abrams K, Leverment J, Spyt T, Waller D & O'Byrne K (2000) Prognostic factors for malignant mesothelioma in 142 patients: validation of CALGB and EORTC prognostic scoring systems. *Thorax* **55**, 731–735.
- 39 Baldini EH, Recht A, Strauss GM, DeCamp MM, Swanson SJ, Liptay MJ, Mentzer SJ & Sugarbaker DJ (1997) Patterns of failure after trimodality therapy for malignant pleural mesothelioma. *Ann Thora Surg* **63**, 334–338.
- 40 Lee DY & Brown EJ (2012) Ubiquilins in the crosstalk among proteolytic pathways. *Biol Chem* **393**, 441–447.
- 41 Yun Lee D, Arnott D & Brown EJ (2013) Ubiquilin4 is an adaptor protein that recruits

Ubiquilin 1 to the autophagy machinery. *EMBO Rep* **14**, 373–381.

Supporting information

Additional supporting information may be found online in the Supporting Information section at the end of the article.

Table S1. GFP competition results of potential ATM substrate candidates.

Table S2. shRNAs sequence.

Table S3. DNA damaging drugs used in this study.

Table S4. The information of patient.